An Experimental Method for Estimating the Tearing Energy in Rubber-like Materials Using the True Stored Energy

Elsiddig Elmukashfi (elsiddig.elmukashfi@eng.ox.ac.uk)
Royal Institute of Technology

Research Article

Keywords: experimental method, tearing energy, true stored energy, materials

Posted Date: January 18th, 2021

DOI: https://doi.org/10.21203/rs.3.rs-144369/v1

Version of Record: A version of this preprint was published at Scientific Reports on August 10th, 2021.
See the published version at https://doi.org/10.1038/s41598-021-95151-y.

An experimental method for estimating the tearing energy in rubber-like materials using the true stored energy

Elsiddig Elmukashfi[1,2,*]

[1]Department of Solid Mechanics, Royal Institute of Technology, Teknikringen 8D, 114 28 Stockholm, Sweden
[2]Department of Engineering Science, University of Oxford, Parks Road, Oxford OX1 3PJ, UK
[*]elsiddig.elmukashfi@eng.ox.ac.uk

ABSTRACT

A method for determining the critical tearing energy in rubber-like materials is proposed. In this method, the energy required for crack propagation in a rubber-like material is determined by the change of the recovered elastic energy. Hence, the dissipated energy due to different inelastic processes is deducted from the total strain energy applied to the system. Therefore, the classical method proposed by Rivlin and Thomas using the pure shear tear test is modified using the actual stored elastic energy. The elastically stored energy in a pure shear is determined experimentally using cyclic loading under quasi-static loading rate of $0.01\ \mathrm{s}^{-1}$ and for different unloading rates, i.e. 0.01, 0.1 and $1.0\ \mathrm{s}^{-1}$. The experimental results show that the classical method overestimates the critical tearing energy by approximately 18% and the unloading rate is minimal which suggests that the dissipation depends only on the loading path.

Introduction

The tearing energy, as a fracture mechanics concept, was proposed by Rivlin and Thomas[1] as an analogy to the energy release rate[2] to study fracture in rubber and rubber-like materials. They assumed that Griffith's approach is valid for the case of large deformation, the irreversible changes in energy due to crack growth take place only in the crack tip vicinity, and the change in energy is independent of the geometry. Therefore, the crack growth is governed by the critical tearing energy criterion that is defined by

$$T_{\mathrm{c}} = -\left.\frac{\partial U}{\partial A}\right|_{\delta_{\mathrm{c}}}, \tag{1}$$

where T_{c} is the critical tearing energy, A is the surface area of one face of the crack, U is the potential energy stored in the system and the suffix $(\bullet)_{\delta_{\mathrm{c}}}$ denotes that the differentiation is carried out at a constant displacement δ_{c}, i.e. the external forces do not produce work. The approach was experimentally verified, concluding that the tearing energy vs. rate of tearing relation is a fundamental material property[1,3–5]. Furthermore, the J-integral approach[6] was later extended to rubber and rubber-like materials by Chang[7] as an alternative approach and the critical J-value (J_{c}) was introduced as equivalence. Moreover, the critical tearing energy has been widely used to study crack initiation and growth in other soft materials such as hydrogels[8] and fibrous biological tissues[9].

Several experimental techniques using different specimens were proposed for determining the critical tearing energy. Rivlin and Thomas[1] introduced the trouser, pure shear, angled and split specimens and since then new specimens have been continuously proposed in the literature, e.g. the single edge notch in tension (SENT)[10], the double cantilever beam (DCB)[11,12], tensile strip test[5,13], the doubly cracked pure shear specimen (DCPS)[14] and the circumferentially-cracked cylindrical specimen (CCC)[15]. The evaluation of the critical tearing energy is generally accomplished by the determination of the potential decrease due to crack growth, i.e. $\partial U/\partial A$. Analytically, in specimens of simple geometries, the tearing energy is obtained from the energy balance assuming that the decrease in potential energy is due to creation of new crack surfaces[1,11,12,14,15]. Other methods are based on constructing a relation between the total energy stored in the system at the crack initiation and the crack length experimentally using specimens with different initial crack length[10,16–18]. These methods assume a purely elastic material and ignore inelastic deformation effects.

Many experimental investigations reveal that rubber and rubber-like materials experience remarkable microstructural changes during deformation such as the development of cavitation damage, breakage of filler-polymer bonds and crystallisation[19–24]. These processes result in inelastic changes including stress softening (Mullins softening effect[25]), hysteresis, permanent set and induced anisotropy. Thus, a significant amount of the strain energy can be dissipated during deformation which may lead to inaccurate estimation of the critical tearing energy. It is worth mentioning that some soft materials experience similar inelastic changes during deformation such as hydrogels and fibrous biological tissues (e.g. see Long and Hui[8] and

Humphrey[26]). In the context of fracture mechanics, Andrews[27] showed, in his theoretical study of an infinite inelastic lamina containing a crack, that the inelastic deformation has a significant role in the total energy change due to crack propagation. Recently, Qi et al.[28] proposed theoretical and computational frameworks to study fracture toughness under steady-state crack propagation assuming neo-Hookean solid with rate-independent hysteresis described by the Mullins effect. However, to the author's knowledge, apart from the work of Qi et al.[28] no experimental correction of the critical tearing energy from the presence of the inelastic changes has been proposed for a stationary crack.

In the present work, a new method for determining the critical tearing energy in rubber and rubber-like materials is introduced. The critical tearing energy is determined from the actual stored elastic energy such that the effect of dissipated energy due to the inelastic deformation is taken into account. The actual stored elastic energy is estimated experimentally using cyclic loading. This method can also be used in other soft materials that experience energy dissipation during loading (i.e. manifested in the form of hysteresis) such as hydrogels and fibrous biological tissues.

Analysis of crack propagation in pure shear tear test

Rivlin and Thomas[1] proposed the pure shear tear test for characterising the tearing energy in rubber-like materials which are assumed to exhibit purely elastic behaviour. In this setup, a pre-cracked pure shear specimen with a low ratio between the height and width is used. A typical specimen is illustrated in Fig. 1 in which the undeformed width, height, and thickness of the specimen are denoted by W_0, H_0 and B_0, respectively, and the crack length by a. The loading is defined by the displacement δ_L and its rate $\dot{\delta}_L$ on the boundary where the applied force is F. Moreover, the critical tearing energy is generally estimated under quasi-static loading conditions (i.e. $\dot{\delta}_L \to 0$) in which the loading rate effects are minimal.

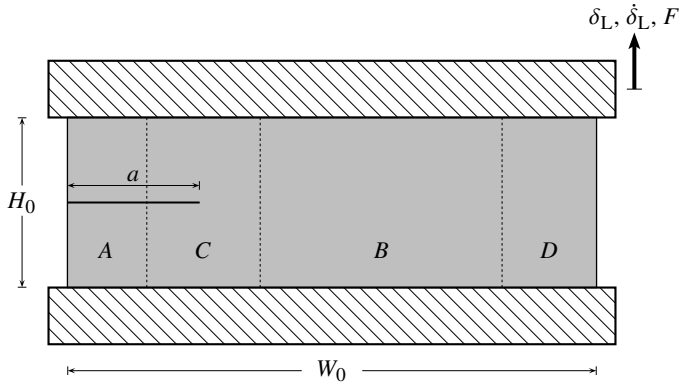

Figure 1. The schematic of the pure shear tear specimen.

The classical method

In order to study the crack propagation, the specimen is divided into four different regions, based on the deformation state: (*i*) region A behind the crack tip in which the material is unloaded, (*ii*) region B is in a state of pure shear deformation, (*iii*) region C, between regions A and B, is in a complicated state of deformation, and (*iv*) region D is between the pure shear region and the traction-free edge. The propagation of the crack is assumed to take place at a fixed separation between the clamps, i.e. $\delta_L = \text{const.}$, and is seen as a shift of region C in the direction of the propagation. Consequently, region A will increase while region B will decrease by the same amount. Hence, the propagation of the crack by $\mathrm{d}a$ (measured in the undeformed configuration) is a process of unloading a volume of $H_0 B_0 \mathrm{d}a$ from the pure shear deformation to the undeformed state. The change of the potential energy $\mathrm{d}U$ in the specimen is defined as

$$\mathrm{d}U = U(a + \mathrm{d}a) - U(a) = -H_0 B_0 \mathrm{d}a \Psi, \tag{2}$$

where Ψ is the elastically stored energy per unit referential volume of the material in a state of pure shear at the critical displacement $\delta_L = \delta_c$ (i.e. at which the crack propagation takes place). It should be noted that the change in the total energy is equal to the change in the elastic stored energy in the case of purely elastic materials. Additionally, the stress-strain state in the vicinity of the crack tip in region C is taken to be self-similar during crack initiation as $\mathrm{d}a \to 0$. Therefore, using Eq. (1),

the critical tearing energy can be determined as

$$T_c = \Psi H_0. \tag{3}$$

The load-displacement relation of a pure shear test under quasi-static loading conditions is assumed to take the general form $F = F(\delta_L, a)$. Therefore, the stored energy per unit referential volume Ψ is obtained by graphical integration under the load-displacement curve of an uncracked pure shear specimen of the material ($a = 0$), see Fig. 2, as

$$\Psi(\delta_c) = \frac{1}{V_0} \int_0^{\delta_c} F(\delta_L, 0)\, d\delta_L, \tag{4}$$

where $V_0 = W_0 H_0 B_0$ is the volume of the specimen in the reference configuration. Strictly speaking, this relation is valid under the assumption of an ideal rubber-like solid in which the deformation is assumed to be purely elastic and the load-displacement relation is reversible.

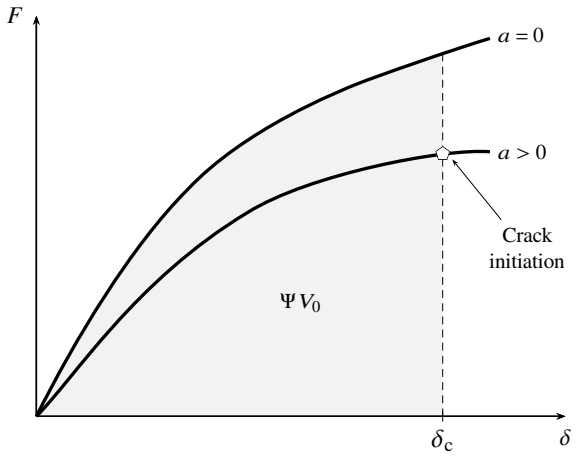

Figure 2. The schematic of the load-displacement curve: the shaded area is the strain energy stored in the uncracked specimen at the critical displacement δ_c.

The modified method

The load-displacement relation for a non ideal rubber-like material in the pure shear test is irreversible and may depend on the unloading rate[29], see Fig. 3. The total change in the total internal energy per unit reference volume of the uncracked pure shear specimen, $\dot{E}$, can be divided into the change in the *elastic* free energy per unit reference volume $\dot{\Psi}$, *heat* and *dissipation* energy per unit reference volume $\dot{Q}$, and *free* energy in other forms per unit reference volume $\dot{\Psi}'$ (e.g. free energy stored as surface energy between the amorphous and crystalline phase during the strain-induced crystallisation):

$$\dot{E} = \dot{\Psi} + \dot{Q} + \dot{\Psi}'. \tag{5}$$

In Figure 4, the elastically stored energy is the area under the unloading curve and the area between the loading and unloading curves is associated with Q and Ψ'. Hence, the actual change in the stored energy due to crack propagation in a pure shear tear specimen is associated with the true elastic energy Ψ rather than the assumed elastic energy.

The irreversible load-displacement relation in a pure shear test can be expressed as $F = F(\delta, \dot{\delta}, a; \boldsymbol{\kappa})$, where δ and $\dot{\delta}$ are the displacement and its rate; and $\boldsymbol{\kappa}$ are some internal variables that describe the different inelastic processes and determine the changes in the load-displacement behaviour. The internal variables, $\boldsymbol{\kappa}$, are history and rate dependent; and can be determined by a set of evolution laws that may take the general form $\dot{\boldsymbol{\kappa}} = \dot{\boldsymbol{\kappa}}(\delta, \dot{\delta}, \Theta, \boldsymbol{\kappa})$, where Θ is the absolute temperature. The actual elastic energy is then obtained by

$$\Psi(\delta_c, \dot{\delta}_U) = \frac{1}{V_0} \int_{\delta_c}^{\delta_p} F(\delta_U, \dot{\delta}_U, 0; \boldsymbol{\kappa})\, d\delta_U, \tag{6}$$

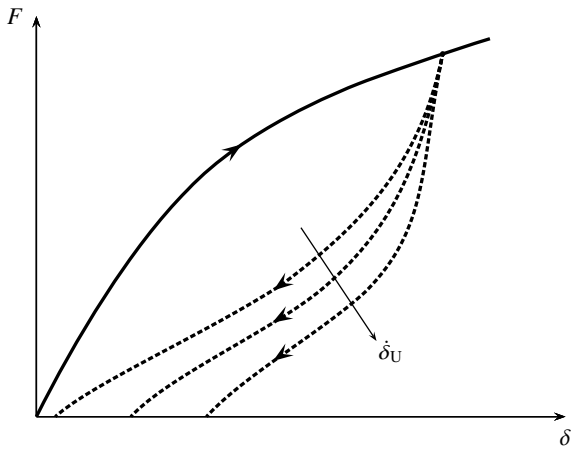

Figure 3. The schematic of the load-displacement curve of a non ideal rubber-like material. The inelastic effects are demonstrated by the irreversibility of the loading-unloading behaviour for different unloading rates $\dot{\delta}_U$.

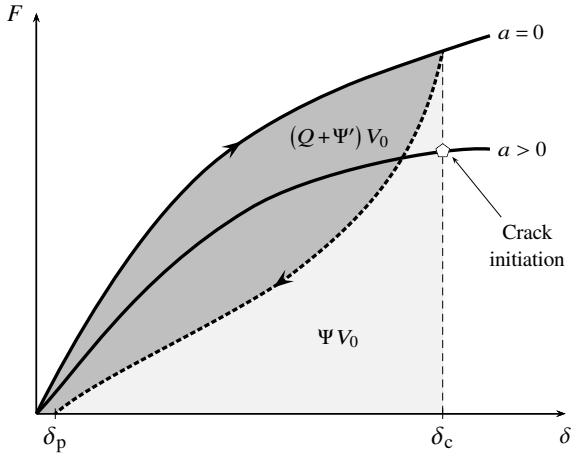

Figure 4. The schematic of the load-displacement curve for a non ideal rubber-like material. The light grey area is the elastic stored energy, ΨV_0, and the dark grey shaded area is the summation of the heat and dissipation energy and the free energy in other forms, $(Q+\Psi')V_0$, in the uncracked specimen at the critical displacement δ_c. δ_p is the permanent deformation after unloading.

and the summation of the heat and dissipation energy becomes

$$Q+\Psi' = \frac{1}{V_0}\oint_0^{\delta_p} F(\delta,\dot{\delta},0;\boldsymbol{\kappa})\,\mathrm{d}\delta, \tag{7}$$

where δ_p is the permanent deformation after the pure shear specimen is completely unloaded and $\boldsymbol{\kappa}$ account for the evolution of inelastic effects during loading and unloading. It should be noted that the forms of the load-displacement and internal variables relations are out of the scope of the current study and we use direct experimental measurements. Further, it is not an easy task to obtain the exact unloading rate of region B during crack growth. Therefore, the unloading rate effect on the recovered elastic energy will be investigated.

Experimental work

A carbon-black-filled natural rubber material is investigated in this experimental study. The material is manufactured by TrelleborgVibracoustic under the designation NR3233 and its chemical properties are listed in Table 1. Two types of specimens have been used in this investigation, i.e. the uncracked and cracked pure-shear specimens. The specimens were of width $W_0 = 110$ mm, height $H_0 = 30$ mm, and thickness $B_0 = 2.5$ mm. In the cracked pure-shear specimens, initial cracks of length $a = 30$ mm were created using razor blades. A standard servo-hydraulic test machine of load capacity 50 KN, was used and the different tests were performed at ambient temperature between 22-25°C and relative humidity 60%. Additionally, a high speed camera at up to 7000 frames/s was used to detect the crack propagation onset. The experiment setup is shown in Fig. 5.

Table 1. The mix formulation in parts per hundred rubber by weight (phr) and Shore A hardness of carbon-black-filled natural rubber (NR3233).

NR	CB	Plasticizer	Additives	Shore A
100	54	13	19	50

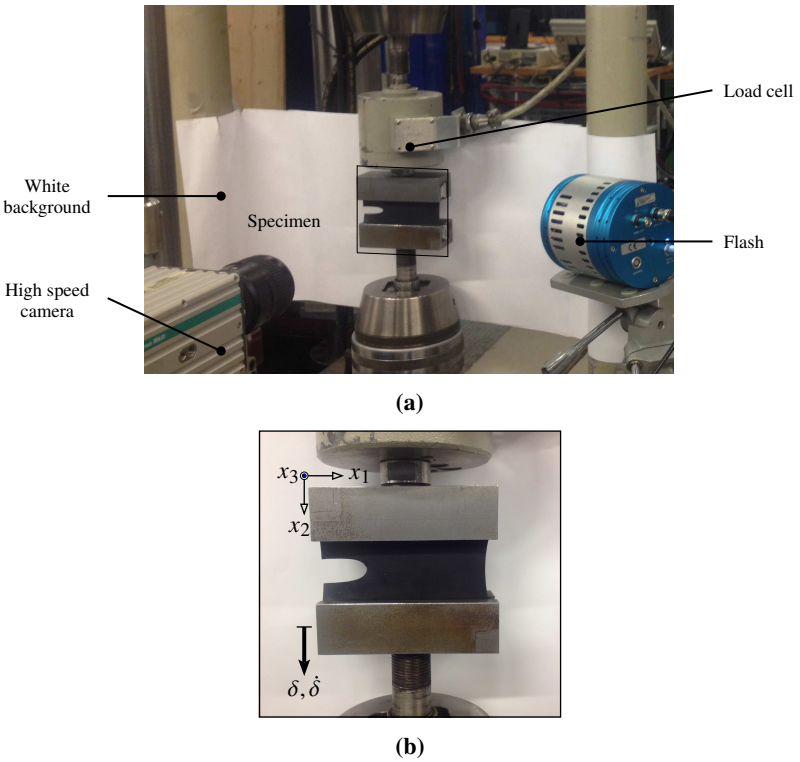

Figure 5. The experimental setup: (a) the loading machine, the cracked pure shear specimen and the high speed camera; (b) the cracked pure shear specimen, the loading direction and the experiment frame.

Four cracked pure-shear specimens were monotonically loaded at cross head speed of 0.3 mm/s until complete failure. It is worth noting that, at this loading rate, the material shows very limited rate sensitivity. The load-displacement graphs were recorded and the crack growth points were marked during the test, and the critical displacement was determined. The uncracked pure-shear specimens were subjected to a cycle of loading and unloading. They were monotonically loaded until the critical displacement, i.e. obtained from the cracked pure-shear specimen, was reached and then they were unloaded completely. The loading cross head speed was kept at 0.3 mm/s (0.01 s^{-1}), as in the case of the cracked specimens. During unloading, the cross head speed was varied to investigate the effect of the unloading rate. Therefore, three unloading cross head speeds were

used, i.e. 0.3, 3.0 and 30.0 mm/s (0.01, 0.1, and 1.0 s^{-1}). Three specimens per unloading rate were tested such that nine specimens were used in total.

Results and Discussion

Fig. 6 shows the load-displacement records of four cracked pure-shear specimens in which the solid circles are the crack initiation points. The average critical displacement is determined to be $\bar{\delta}_c = 13.131$ mm with a standard deviation of 1.897 mm which corresponds to the average stretch $\bar{\lambda}_c = 1.44$.

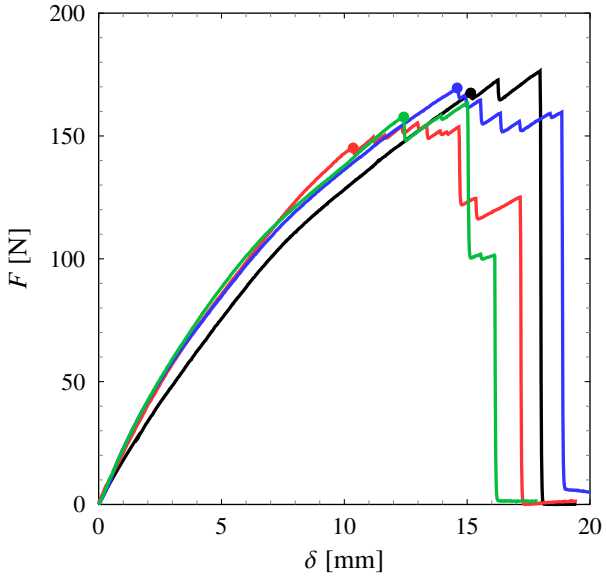

Figure 6. The load-displacement curves of four cracked pure-shear specimens where the solid circles denote the crack initiation points.

Typical load-displacement records for an uncracked pure-shear specimen are shown in Fig. 7, wherein the specimens are loaded under controlled deformation until the average critical displacement $\bar{\delta}_c$ and then unloaded. The material shows nonlinear large deformation behaviour and significant energy dissipation.
The total energy E and actual elastic energy Ψ per unit volume were evaluated numerically using the load-displacement records of the uncracked pure-shear specimens at different unloading rates. The critical tearing energy was then determined using the classical and proposed methods using Eqs (4) and (6), respectively; together with Eq (3). Using the classical method, the critical tearing energy is found to be $\bar{T}_c = 7.04\,\mathrm{kJ/m^2}$ with a standard deviation of $1.64\,\mathrm{kJ/m^2}$. Table 2 shows the critical tearing energies using the true stored elastic energy at different unloading rates $\dot{\delta}_U$. The result suggests that the classical method overestimates the critical tearing energy by $\approx 18\%$. Further, the recovered elastic energy is independent of the unloading rate from the experimental range which indicates that the heat and dissipation and/or the free energy depend only on the loading path. The experimental studies on Mullins effect yield that the dissipation increases progressively with the increasing stretch, the filler content, crystallisation and damage[30]. Hence, the recovered elastic energy depend on the material, loading rate and the critical stretch λ_c.

Conclusions

In conclusion, a modified method for estimation of the critical tearing energy in rubber-like solids has been presented. The method is a modification of the classical method proposed by Rivlin and Thomas[1] using the pure shear tear test. In this method, the total energy stored in a rubber-like material is divided into elastic and inelastic contributions taking into account the different inelastic processes. Hence, the energy required for crack propagation is determined by the change of the elastically stored energy only rather that the total energy in the case of the classical method. Strictly speaking, the stress-strain state in

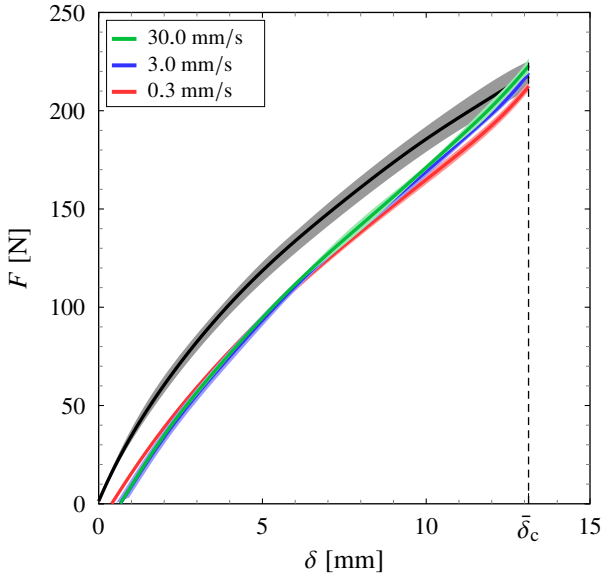

Figure 7. The load-displacement curves of uncracked pure-shear specimens at loading rate of 0.3 mm/s (0.01 s^{-1}) and different unloading rates. The red, blue and green lines represent the unloading rates of 0.3, 3.0, and 30.0 mm/s (i.e. 0.01, 0.1, and 1.0 s^{-1}), respectively, and fill areas represent the experiment scatter (error bars). The unloading point is taken at $\bar{\delta}_c = 13.131$ mm.

Table 2. The average critical tearing energy $\bar{T}_c$ and its standard deviation $\tilde{\sigma}_{T_c}$ using the true stored elastic energy for different unloading rates $\dot{\lambda}_U$.

$\dot{\lambda}_U$ [s^{-1}]	$\bar{T}_c$ [kJ/m^2]	$\tilde{\sigma}_{T_c}$ [kJ/m^2]
0.01	5.95	1.50
0.1	5.98	1.60
1.0	6.06	1.74

the vicinity of the crack tip is taken to be self-similar during crack initiation as $da \to 0$. The experimental investigations of carbon-black-filled natural rubber material show that a significant amount of energy is dissipated during deformation which results in an overestimation of the critical tearing energy by $\approx 18\%$. The recovered elastic energy does not depend on the unloading rate for the range $0.01 - 1.0\ s^{-1}$ and depend only on the loading path. Therefore, to accurately measure the critical tearing energy, the recovered elastic energy should be experimentally measured which depend on the material, loading rate and the critical stretch λ_c. The proposed method should be used to study other soft materials that experience energy dissipation during loading such as hydrogels and fibrous biological tissues. Additionally, similar approach can be used to estimate the actual tearing in specimens of simple geometries such as the trouser and single edge notch in tension (SENT) specimens.

Acknowledgement

The author is grateful for valuable discussions with Professor Martin Kroon. The author would like also to thank Dr. Rickard Österlöf for providing the material, Mr. kurt Lindqvist and Mr. Göran Rådberg for helping in manufacturing the specimens, and M.Sc. Martin Öberg and Dr. Irene Arregui for their assistance during the experimental realisation of this work.

References

1. Rivlin, R. & Thomas, A. Rupture of rubber. I. characteristic energy for tearing. *J. Polym. Sci.* **10**, 291–318 (1953).
2. Griffith, A. The phenomena of rupture and flow in solids. *Philos. transactions royal society london. Ser. A, containing papers a mathematical or physical character* **221**, 163–198 (1921).
3. Greensmith, H. & Thomas, A. Rupture of rubber. III. determination of tear properties. *Rubber Chem. Technol.* **29**, 372–381 (1956).
4. Thomas, A. Rupture of rubber. VI. further experiments on the tear criterion. *J. Appl. Polym. Sci.* **3**, 168–174 (1960).
5. Lake, G., Thomas, A., Lake, G. & Thomas, A. The strength of highly elastic materials. *Proc. Royal Soc. London. Ser. A. Math. Phys. Sci.* **300**, 108–119 (1967).
6. Rice, J. R. A path independent integral and the approximate analysis of strain concentration by notches and cracks. *J. applied mechanics* **35**, 379–386 (1968).
7. Chang, S.-J. Path-independent integral for rupture of perfectly elastic materials. *Zeitschrift für angewandte Math. und Physik ZAMP* **23**, 149–152 (1972).
8. Long, R. & Hui, C.-Y. Fracture toughness of hydrogels: measurement and interpretation. *Soft Matter* **12**, 8069–8086 (2016).
9. Bircher, K., Zündel, M., Pensalfini, M., Ehret, A. E. & Mazza, E. Tear resistance of soft collagenous tissues. *Nat. communications* **10**, 1–13 (2019).
10. Hocine, N. A., Abdelaziz, M. N. & Mesmacque, G. Experimental and numerical investigation on single specimen methods of determination of J in rubber materials. *Int. journal fracture* **94**, 321–338 (1998).
11. South, J. T., Case, S. W. & Reifsnider, K. L. Crack growth of natural rubber using a modified double cantilever beam. *Mech. materials* **34**, 451–458 (2002).
12. Nilsson, F. Large displacement aspects on fracture testing with double cantilever beam specimens. *Int. journal fracture* **139**, 305–311 (2006).
13. Lake, G., Lawrence, C. & Thomas, A. High-speed fracture of elastomers: Part I. *Rubber chemistry technology* **73**, 801–817 (2000).
14. Mazich, K. A., Morman, K., Oblinger, F., Fan, T. & Killgoar Jr, P. The effect of specimen thickness on the tearing energy of a gum vulcanizate. *Rubber chemistry technology* **62**, 850–862 (1989).
15. Morman Jr, K., Mazich, K., Oblinger, F., Zhang, F. & Killgoar Jr, P. Critical tearing energy in a circumferentially-cracked circular cylinder of rubber under finite deformation. *Int. journal fracture* **53**, 129–157 (1992).
16. Kim, B. & Joe, C. A method to evaluate critical J-integral value: locus method. *Polym. testing* **7**, 355–363 (1987).
17. Kim, B. & Joe, C. Single specimen test method for determining fracture energy (J_c) of highly deformable materials. *Eng. fracture mechanics* **32**, 155–161 (1989).
18. Joe, C. & Kim, B. A method to determine the R-curve of flexible materials using a monotonic loading of a single trouser tear specimen. *Int. journal fracture* **44**, 15–26 (1990).
19. Gent, A. & Lindley, P. Internal rupture of bonded rubber cylinders in tension. *Proc. Royal Soc. London. Ser. A. Math. Phys. Sci.* **249**, 195–205 (1959).
20. Williams, M. & Schapery, R. Spherical flaw instability in hydrostatic tension. *Int. J. Fract. Mech.* **1**, 64–72 (1965).
21. Payne, A. R. The dynamic properties of carbon black-loaded natural rubber vulcanizates. part I. *J. applied polymer science* **6**, 57–63 (1962).
22. Payne, A. A note on the conductivity and modulus of carbon black-loaded rubbers. *J. Appl. Polym. Sci.* **9**, 1073–1082 (1965).
23. Andrews, E. Spherulite morphology in thin films of natural rubber. *Proc. Royal Soc. London. Ser. A. Math. Phys. Sci.* **270**, 232–241 (1962).
24. Andrews, E., Owen, P. & Singh, A. Microkinetics of lamellar crystallization in a long chain polymer. *Proc. Royal Soc. London. A. Math. Phys. Sci.* **324**, 79–97 (1971).
25. Mullins, L. Effect of stretching on the properties of rubber. *Rubber Chem. Technol.* **21**, 281–300 (1948).

26. Humphrey, J. D. Continuum biomechanics of soft biological tissues. *Proc. Royal Soc. London. Ser. A: Math. Phys. Eng. Sci.* **459**, 3–46 (2003).

27. Andrews, E. A generalized theory of fracture mechanics. *J. Mater. Sci.* **9**, 887–894 (1974).

28. Qi, Y., Caillard, J. & Long, R. Fracture toughness of soft materials with rate-independent hysteresis. *J. Mech. Phys. Solids* **118**, 341–364 (2018).

29. Carleo, F., Barbieri, E., Whear, R. & Busfield, J. J. Limitations of viscoelastic constitutive models for carbon-black reinforced rubber in medium dynamic strains and medium strain rates. *Polymers* **10**, 988 (2018).

30. Diani, J., Fayolle, B. & Gilormini, P. A review on the mullins effect. *Eur. Polym. J.* **45**, 601–612 (2009).

Figures

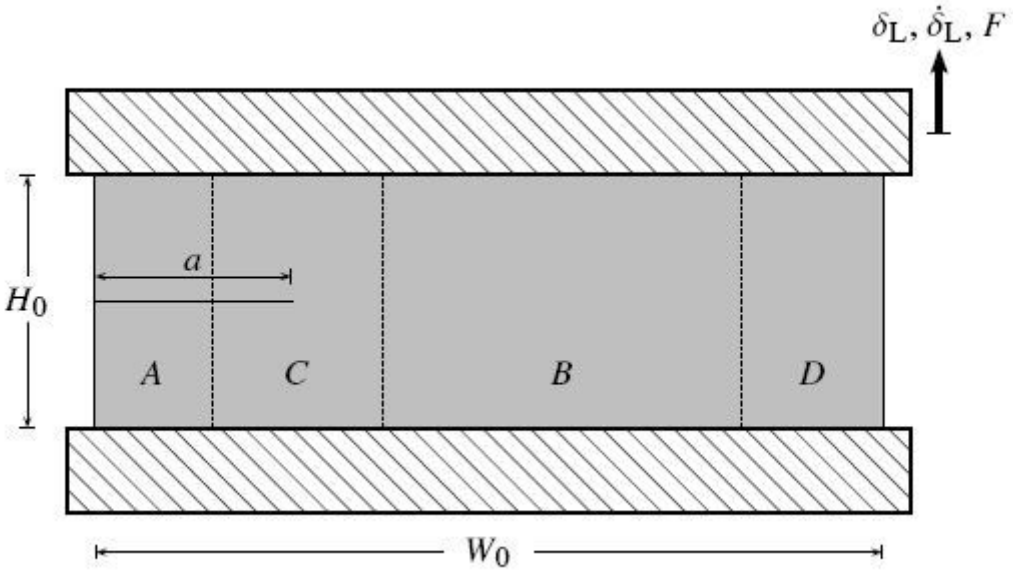

Figure 1

The schematic of the pure shear tear specimen.

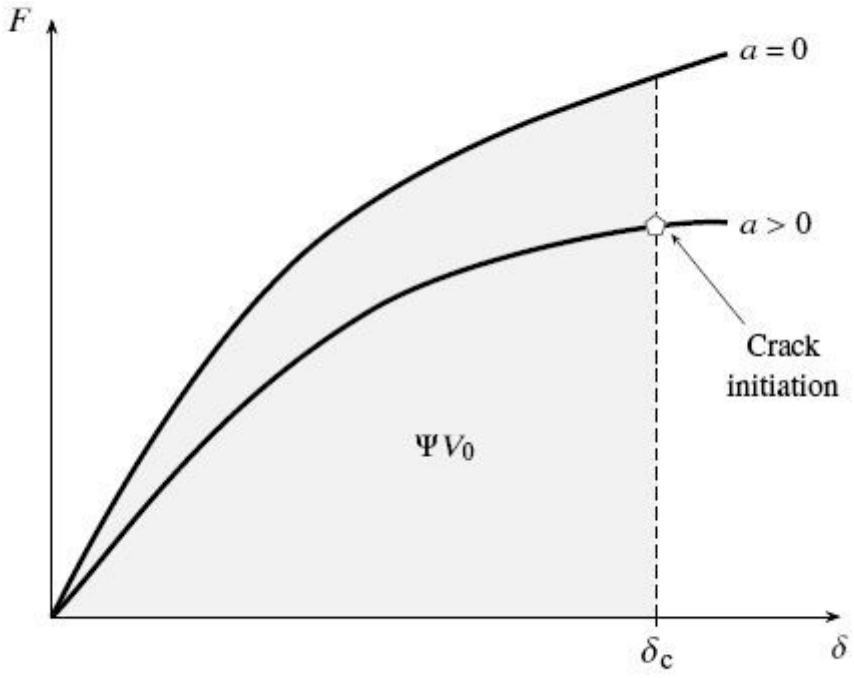

Figure 2

The schematic of the load-displacement curve: the shaded area is the strain energy stored in the uncracked specimen at the critical displacement δc.

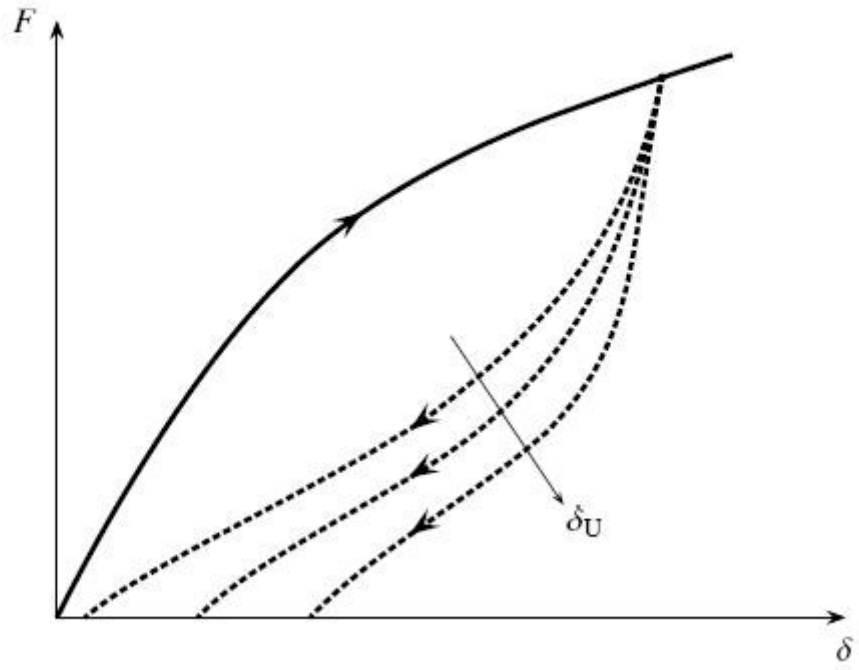

Figure 3

The schematic of the load-displacement curve of a non ideal rubber-like material. The inelastic effects are demonstrated by the irreversibility of the loading-unloading behaviour for different unloading rates δU.

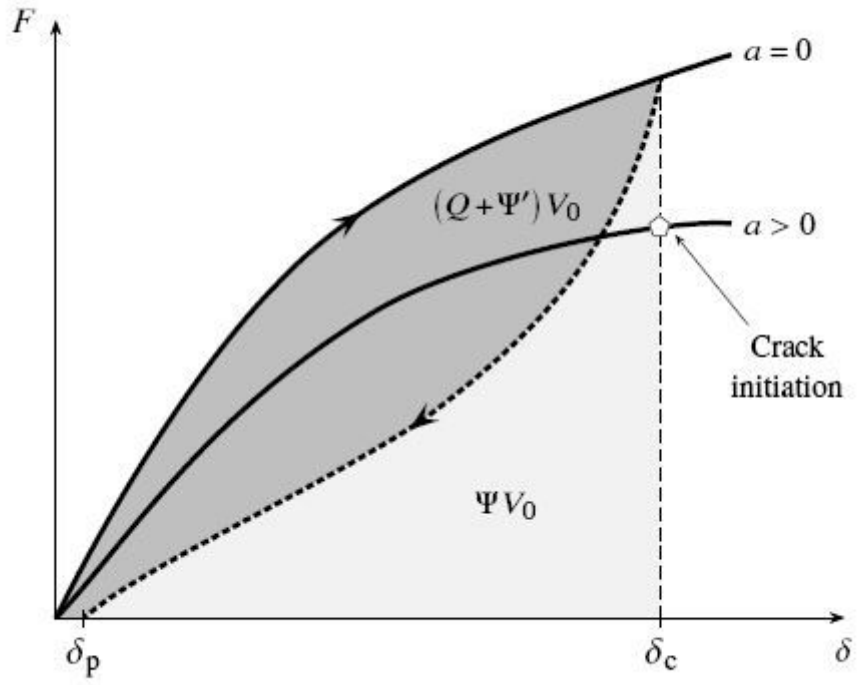

Figure 4

The schematic of the load-displacement curve for a non ideal rubber-like material. The light grey area is the elastic stored energy, ΨV0, and the dark grey shaded area is the summation of the heat and dissipation energy and the free energy in other forms, (Q+Ψ')V0, in the uncracked specimen at the critical displacement δc. δp is the permanent deformation after unloading.

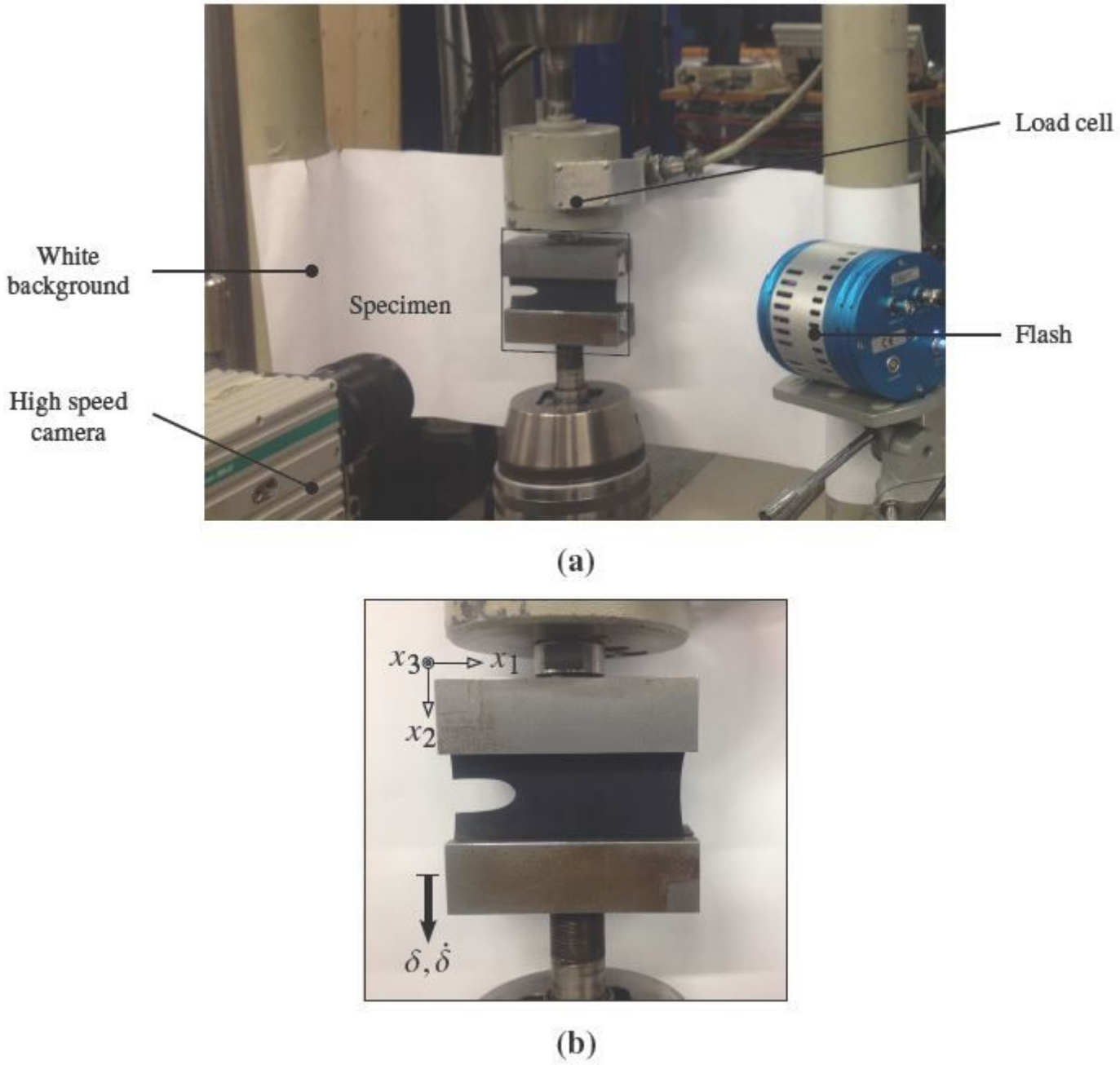

Figure 5

The experimental setup: (a) the loading machine, the cracked pure shear specimen and the high speed camera; (b) the cracked pure shear specimen, the loading direction and the experiment frame.

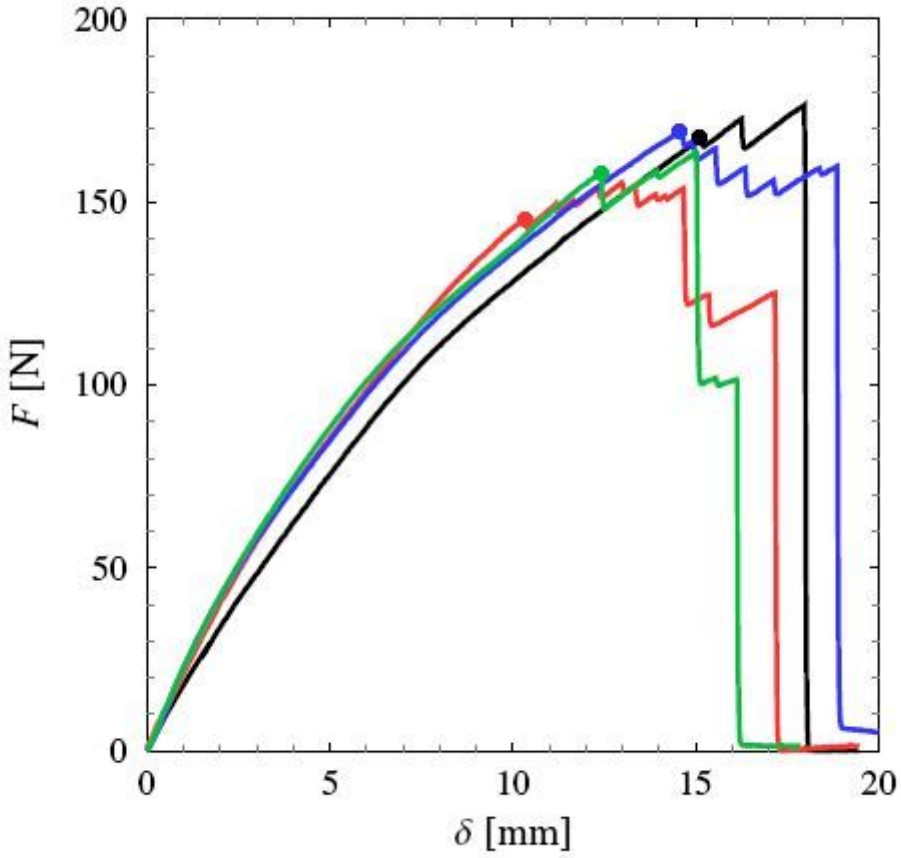

Figure 6

The load-displacement curves of four cracked pure-shear specimens where the solid circles denote the crack initiation points.

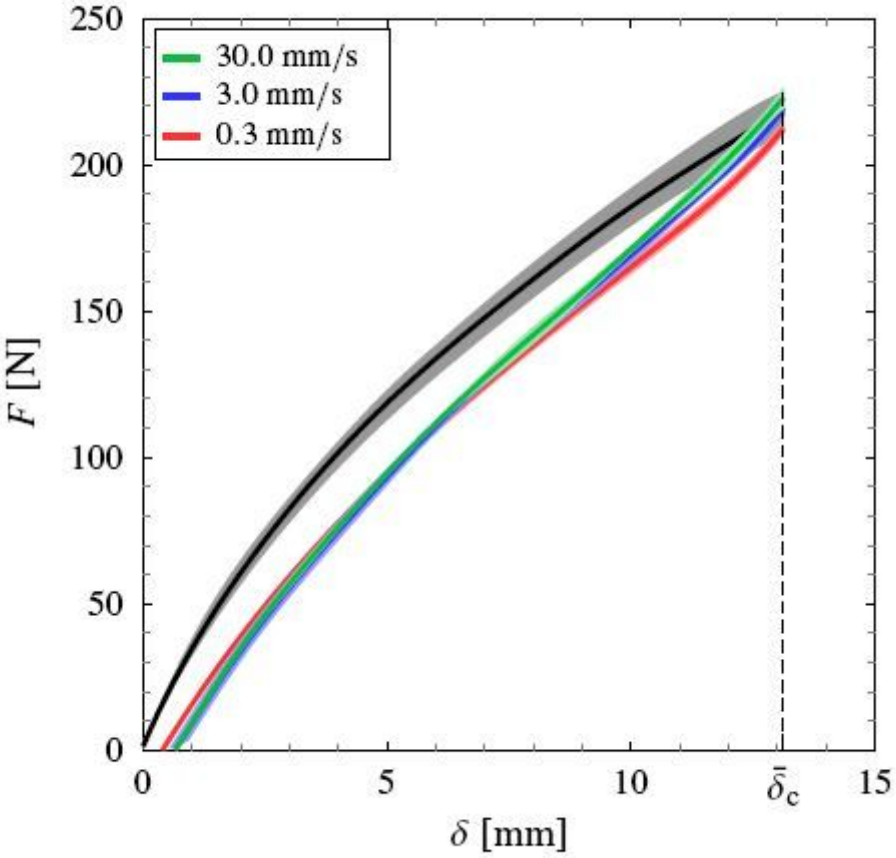

Figure 7

The load-displacement curves of uncracked pure-shear specimens at loading rate of 0.3 mm/s (0.01 s−1) and different unloading rates. The red, blue and green lines represent the unloading rates of 0.3, 3.0, and 30.0 mm/s (i.e. 0.01, 0.1, and 1.0 s−1), respectively, and fill areas represent the experiment scatter (error bars). The unloading point is taken at $\bar{\delta}_c$ = 13.131 mm.